

Error-tolerant parity detector of cat-state qubits based on a topological quantum phase transition

Yi-Hao Kang , Yu Wang , Qi-Ping Su , Guo-Qiang Zhang, Wei Feng , and Chui-Ping Yang 

School of Physics, Hangzhou Normal University, Hangzhou 311121, China



(Received 29 May 2024; accepted 12 July 2024; published 30 July 2024)

We propose a scheme for realizing parity measurement of cat-state qubits based on a topological quantum phase transition. The cat-state qubits, formed by the bosonic modes in the Kerr-nonlinear resonators with two-photon squeezing drives, couple with a superconducting qubit in the center. We demonstrate that the resonator-qubit couplings with proper strengths can induce a topological quantum phase transition when the cat-state qubits are initial in the even-parity states. The topological quantum phase transition provides an approach to distinguish the even-parity states from the odd-parity states by measuring a topological invariant, namely the Chern number. Due to the robustness of the Chern number, the scheme shows great tolerance for multiple types of disturbing factors, including the systematic errors of the control fields and the coupling strengths, the inter-resonator crosstalk, and decoherence. Therefore, the scheme may be useful to construct an error-tolerant parity detector of cat-state qubits.

DOI: [10.1103/PhysRevA.110.012463](https://doi.org/10.1103/PhysRevA.110.012463)

I. INTRODUCTION

Parity measurement plays an important role in quantum information processing [1–6]. It has shown applications in quantum information tasks, including quantum computation [7–9], entanglement swapping [10–12], quantum teleportation [13–15], entanglement purification [16–19], and quantum error correction [20–22]. Motivated by the abundant applications of parity measurement, much effort has been devoted to constructing parity detectors in various physical systems. To date, effective parity detectors for the physical qubits, including photonic qubits [23,24], atomic qubits [25,26], spin qubits [27], and superconducting qubits [28–30], have been reported.

In recent years, logical qubits [31–37], which provide protection of quantum information from noise and decoherence, have drawn much attention in fault-tolerant quantum computation. The cat-state qubits are one kind of useful logical qubits [38–43]. In the basis of the even and odd cat states, the phase-shift errors are exponentially suppressed [44–46]. Hence, one can only focus on the bit-flip errors in a quantum error correction [47]. Attracted by the advantages of the cat-state qubits, many schemes have been proposed to realize quantum computation with cat-state qubits [48–53]. To further stimulate quantum information processing based on cat-state qubits, it is necessary to construct parity detectors for cat-state qubits.

Until now, several schemes [54,55] have been put forward to measure the parity of the cat-state qubits via selective population transfers of an auxiliary qubit. However, the populations of the target states are usually sensitive to errors of control parameters and decoherence [56,57]. More specifically, the

populations of the target states can hardly maintain unity in the presence of parametric errors and decoherence, which makes these schemes [54,55] fail if the wrong final states are reported. To enhance the robustness of the parity measurement, robust criteria should be considered for a parity measurement instead of the populations. Fortunately, previous works have shown that some topological invariants, such as the Chern number, remain unchanged by small perturbations to the system [58–63]. The jumps in the values of these topological invariants represent nontrivial quantum topological phase transitions [58,62]. These works give us a clue to achieve error-tolerant parity measurement via topological quantum phase transition.

In this paper, we propose a scheme to build a parity detector of cat-state qubits based on topological quantum phase transition. The cat-state qubits are formed by the bosonic modes in the Kerr-nonlinear resonators driven by two-photon squeezing drives. We couple the resonators with a superconducting qubit in the center and demonstrate that the resonator-qubit couplings can be tuned to induce a topological quantum phase transition when the cat-state qubits are initial in the even-parity states. The topological quantum phase transition allows us to distinguish the even-parity states from the odd-parity states by measuring a topological invariant, i.e., the Chern number. Benefiting from the robustness of the Chern number, the scheme is insensitive to various disturbing factors, including the systematic errors of the control fields and the coupling strengths, the inter-resonator crosstalk, and decoherence. Therefore, the scheme may provide an effective approach to construct an error-tolerant parity detector of cat-state qubits.

II. PHYSICAL MODEL

We consider a physical model containing two Kerr-nonlinear resonators $\{C_n | n = 1, 2\}$ driven by two-photon

*Contact author: 20426399@qq.com

[†]Contact author: yangcp@hznu.edu.cn

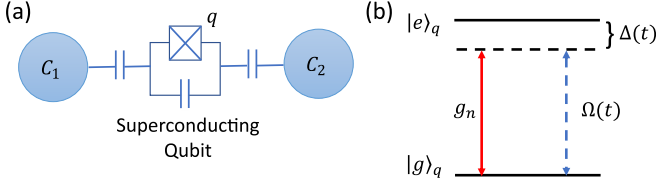


FIG. 1. (a) Diagrammatic sketch of the physical model for the parity detector of cat-state qubits based on topological quantum phase transition. The cat-state qubit n is formed by the mode in the resonator C_n ($n = 1, 2$) coupling with the auxiliary superconducting qubit q in the center. (b) Level configuration of the auxiliary superconducting qubit q driven by a classical field with Rabi frequency $\Omega(t)$ and coupled with the resonator C_n with coupling strength g_n .

squeezing drives and coupled with an auxiliary superconducting qubit q , as shown in Fig. 1. The frequencies of the resonator C_n and its corresponding two-photon squeezing drive are assumed as ω_n and $2\omega_n$. The self-Hamiltonian of the Kerr-nonlinear resonator C_n in the frame rotating at the resonator frequency ω_n is (setting $\hbar = 1$) [64–66]

$$H_n = -K_n a_n^{\dagger 2} a_n^2 + \varepsilon_n a_n^{\dagger 2} + \varepsilon_n^* a_n^2, \quad (1)$$

with the Kerr nonlinearity K_n of the resonator C_n , the strength ε_n of the two-photon squeezing drive applied to the resonator C_n , and the creation (annihilation) operator a_n^\dagger (a_n) of the resonator C_n . The resonator C_n couples with the transition $|g\rangle_q \leftrightarrow |e\rangle_q$ of the qubit q with the coupling strength g_n . In addition, the transition $|g\rangle_q \leftrightarrow |e\rangle_q$ of the qubit q is driven by a classical field with Rabi frequency $\Omega(t)$ and frequency ω . We consider the frequency matching as $\omega_n = \omega$, and suppose that the $|g\rangle_q \leftrightarrow |e\rangle_q$ transition frequency of the qubit q is modulated as $\omega_e(t) = \omega + \Delta(t)$. In the frame rotating at the frequency ω , the interaction Hamiltonian of the qubit q and the two resonators is

$$H_q = \left[\Omega(t) + \sum_{n=1,2} g_n a_n^\dagger \right] |g\rangle_q \langle e| + \text{H.c.} + \Delta(t) |e\rangle_q \langle e|. \quad (2)$$

The total Hamiltonian of the system reads $H_{\text{tot}} = H_q + \sum_{n=1}^2 H_n$.

For $\varepsilon_n = K_n \alpha^2$, the even cat state $|\mathcal{C}_+\rangle_n$ and the odd cat state $|\mathcal{C}_-\rangle_n$, defined by

$$|\mathcal{C}_\pm\rangle_n = \frac{1}{\sqrt{\mathcal{N}_\pm}} (|\alpha\rangle_n \pm |-\alpha\rangle_n), \quad (3)$$

are the two lowest orthonormal degenerate eigenvectors of the Hamiltonian H_n . Here, $\mathcal{N}_\pm = 2[1 \pm \exp(-2|\alpha|^2)]$ are the normalized coefficients, and $|\pm\alpha\rangle_n$ are the coherence states of the mode in the resonator C_n with the complex amplitude $\pm\alpha$. For $|\alpha| \gg 1$, the cat states are separated from the rest of the spectrum by an energy gap $E_{\text{gap}} \simeq 4K|\alpha|^2$ [66]. When the energy gap satisfies $E_{\text{gap}} \gg g_n$, the evolution of the resonator C_n can be restricted in the cat-state subspace spanned by $\{|\mathcal{C}_\pm\rangle_n\}$. Thus, a cat-state qubit can be constructed.

In the basis of $\{|\mathcal{C}_\pm\rangle_n\}$, the annihilation operator a_n can be rewritten as

$$\begin{aligned} a_n &= \left(\sum_{i=\pm} |\mathcal{C}_i\rangle_n \langle \mathcal{C}_i| \right) a_n \left(\sum_{i'=\pm} |\mathcal{C}_{i'}\rangle_n \langle \mathcal{C}_{i'}| \right) \\ &= \frac{2\alpha}{\sqrt{\mathcal{N}_+ \mathcal{N}_-}} \sigma_{x,n} - \frac{2i\alpha}{\sqrt{\mathcal{N}_+ \mathcal{N}_-}} e^{-2|\alpha|^2} \sigma_{y,n}, \end{aligned} \quad (4)$$

with $\sigma_{x,n} = |\mathcal{C}_+\rangle_n \langle \mathcal{C}_-| + \text{H.c.}$, $\sigma_{y,n} = -i|\mathcal{C}_+\rangle_n \langle \mathcal{C}_-| + \text{H.c.}$, and $\sigma_{z,n} = |\mathcal{C}_+\rangle_n \langle \mathcal{C}_+| - |\mathcal{C}_-\rangle_n \langle \mathcal{C}_-|$. When $|\alpha| \gg 1$, we obtain $a_n \simeq \alpha \sigma_{x,n}$. Assuming $g_n = g$ and $\text{Im}(g\alpha^*) = 0$, the effective Hamiltonian of the whole system of the cat-state qubits 1 and 2 and the qubit q can be derived as

$$\begin{aligned} H_{\text{eff}} &= \text{Re}[\Omega(t)]\sigma_x + \text{Im}[\Omega(t)]\sigma_y + \Delta(t)\sigma_z/2 \\ &\quad + 2g\alpha^*(|\Psi_+\rangle_{1,2} \langle \Phi_+| + \text{H.c.})\sigma_x, \end{aligned} \quad (5)$$

with $\sigma_x = |e\rangle_q \langle g| + \text{H.c.}$, $\sigma_y = -i|e\rangle_q \langle g| + \text{H.c.}$, and $\sigma_z = |e\rangle_q \langle e| - |g\rangle_q \langle g|$. Here, the term $\Delta(t)(|e\rangle_q \langle e| + |g\rangle_q \langle g|)/2$ is omitted as it is proportional to the identity operator of the qubit q . In addition, the Bell-state vectors for the cat-state qubits 1 and 2 are given by

$$\begin{aligned} |\Phi_\pm\rangle_{1,2} &= \frac{1}{\sqrt{2}} (|\mathcal{C}_+\rangle_1 |\mathcal{C}_+\rangle_2 \pm |\mathcal{C}_-\rangle_1 |\mathcal{C}_-\rangle_2), \\ |\Psi_\pm\rangle_{1,2} &= \frac{1}{\sqrt{2}} (|\mathcal{C}_+\rangle_1 |\mathcal{C}_-\rangle_2 \pm |\mathcal{C}_-\rangle_1 |\mathcal{C}_+\rangle_2). \end{aligned} \quad (6)$$

Defining

$$|\tilde{\Psi}_\pm\rangle_{1,2} = \frac{1}{\sqrt{2}} (|\Phi_\pm\rangle_{1,2} \pm |\Psi_\pm\rangle_{1,2}), \quad (7)$$

the effective Hamiltonian in Eq. (5) can be diagonalized as

$$\begin{aligned} H_{\text{eff}} &= \text{Re}[\Omega(t)]\sigma_x + \text{Im}[\Omega(t)]\sigma_y + \Delta(t)\sigma_z/2 \\ &\quad + 2g\alpha^*(|\tilde{\Psi}_+\rangle_{1,2} \langle \tilde{\Psi}_+| - |\tilde{\Psi}_-\rangle_{1,2} \langle \tilde{\Psi}_-|)\sigma_x. \end{aligned} \quad (8)$$

III. PARITY MEASUREMENT OF CAT-STATE QUBITS BASED ON A TOPOLOGICAL QUANTUM PHASE TRANSITION

A. Introduction of the Berry connection, the Berry curvature, and the Chern number

Let us first review the Berry connection, the Berry curvature, and the Chern number used in characterizing the topological quantum phase transition for the parity measurement. We consider a system with the Hamiltonian H , which has a nondegenerate eigenvector denoted by $|\psi\rangle$. During the adiabatic evolution along the eigenvector $|\psi\rangle$ around a closed path denoted by a vector $\vec{s} = [s_1, s_2, \dots]$ in a parameter space, apart from the dynamic phase, it has been shown that there is an additional phase contribution, which is known as the Berry phase [67]. The Berry phase Θ can be obtained by the integral [61,67]

$$\Theta = \oint_s \vec{A} \cdot d\vec{s}, \quad (9)$$

along the path \vec{s} . Here, $\vec{A} = i\langle\psi|\nabla|\psi\rangle$ is called the Berry connection, the μ th component of which is

$$A_\mu = i\langle\phi|\frac{\partial}{\partial s_\mu}|\phi\rangle. \quad (10)$$

From the Stokes theorem, the Berry phase Θ can also be given by the surface integral [61,68]

$$\Theta = \iint_{\mathcal{S}_s} \vec{B} \cdot d\vec{S} = \iint_{\mathcal{S}_s} B_{\mu\nu} dS_{\mu\nu}, \quad (11)$$

over the area \mathcal{S}_s enclosed by the path \vec{s} . Here, $dS_{\mu\nu} = ds_\mu \wedge ds_\nu$ is the area form element, and \wedge denotes the wedge product. In Eq. (11), \vec{B} is called the Berry curvature, whose component is given by [68]

$$B_{\mu\nu} = \frac{\partial}{\partial s_\mu} A_\nu - \frac{\partial}{\partial s_\nu} A_\mu. \quad (12)$$

The Berry curvature characterizes how the eigenvector is modified by changing parameters [62]. If the path \vec{s} lies on a closed manifold \mathcal{S} , the integral of the Berry curvature over the manifold \mathcal{S} gives a well-defined topological invariant known as the (first) Chern number [69]

$$\mathcal{C} = \frac{1}{2\pi} \iint_{\mathcal{S}} B_{\mu\nu} dS_{\mu\nu}, \quad (13)$$

which is quantized to integer values [62,70].

To date, the Berry phase, the Chern number, and the related concepts have shown multiple applications in many different quantum and classical systems. For example, the Chern number has been exploited in the quantization of the resistance in the integer quantum Hall effect [58–60,71]. The Berry phase and the Chern number also appear in anomalous quantum Hall effect in magnetic metals [72] and the transport in graphene in a quantum Hall regime [73]. In addition, they also emerge in photon interference of a circularly polarized light [74], Thouless pumps [75,76], bianisotropic material [77], and geometric quantum computation [78,79]. Moreover, recent studies have shown that the Berry phase, the Berry connection, the Berry curvature, and the Chern number are exploited in the observation of topological quantum phase transitions in various physical systems [80–85].

B. The parity operator and the expressions of the even-parity and odd-parity states

We define the parity operator for the cat-state qubits 1 and 2 as $P_{1,2} = \sigma_{z,1} \otimes \sigma_{z,2}$. The even-parity and the odd-parity states can be described as

$$\begin{aligned} |\Psi_e\rangle &= \beta_1|\Phi_+\rangle_{1,2} + \beta_2|\Phi_-\rangle_{1,2}, \\ |\Psi_o\rangle &= \beta_3|\Psi_+\rangle_{1,2} + \beta_4|\Psi_-\rangle_{1,2}, \end{aligned} \quad (14)$$

with $|\beta_1|^2 + |\beta_2|^2 = |\beta_3|^2 + |\beta_4|^2 = 1$, which are the eigenvectors of the parity operator $P_{1,2}$ with the eigenvalues 1 and -1 , respectively. Introducing a Hadamard gate \mathcal{H}_n on the cat-state qubit n as (in the basis $\{|\mathcal{C}_\pm\rangle\}$)

$$\mathcal{H}_n = \frac{1}{\sqrt{2}} \begin{bmatrix} 1 & 1 \\ 1 & -1 \end{bmatrix}, \quad (15)$$

the even-parity and the odd-parity states are respectively transformed into

$$\begin{aligned} |\Phi_e\rangle &= \mathcal{H}_1 \mathcal{H}_2 |\Psi_e\rangle = \tilde{\beta}_+ |\tilde{\Psi}_+\rangle_{1,2} + \tilde{\beta}_- |\tilde{\Psi}_-\rangle_{1,2}, \\ |\Phi_o\rangle &= \mathcal{H}_1 \mathcal{H}_2 |\Psi_o\rangle = \beta_3 |\Phi_-\rangle_{1,2} - \beta_4 |\Psi_-\rangle_{1,2}, \end{aligned} \quad (16)$$

with $\tilde{\beta}_\pm = (\beta_1 \pm \beta_2)/\sqrt{2}$. The Hadamard gate \mathcal{H}_n in Eq. (15) can be readily realized in a Kerr-nonlinear resonator, which is shown in the Appendix.

In the following, let us show that the parity of the cat-state qubits 1 and 2 can be distinguished based on a topological quantum phase transition by using the effective Hamiltonian in Eq. (8), after the Hadamard gates \mathcal{H}_1 and \mathcal{H}_2 . Here, the control parameters are parametrized as

$$\begin{aligned} \text{Re}[\Omega(t)] &= -r \cos \theta, \\ \text{Im}[\Omega(t)] &= r \sin \theta \cos \varphi, \\ \Delta(t) &= 2r \sin \theta \sin \varphi. \end{aligned} \quad (17)$$

C. The Chern number in the odd-parity case

When the cat-state qubits 1 and 2 are initial in the odd-parity state $|\Psi_o\rangle$, after the Hadamard gates $\{\mathcal{H}_n|n=1,2\}$ in Eq. (15), they evolve to the state $|\Phi_o\rangle$ in Eq. (16). As the state $|\Phi_o\rangle$ is orthogonal to the states $|\tilde{\Psi}_\pm\rangle_{1,2}$, the last term of the effective Hamiltonian H_{eff} in Eq. (8) can be omitted. In this case, the evolution of the qubit q is governed by the Hamiltonian

$$H_{q,o} = -r \cos \theta \sigma_x + r \sin \theta \cos \varphi \sigma_y + r \sin \theta \sin \varphi \sigma_z. \quad (18)$$

The eigenvectors of the Hamiltonian $H_{q,o}$ in the basis $\{|e\rangle_q, |g\rangle_q\}$ read

$$\begin{aligned} |\phi(\theta, \varphi)\rangle &= \frac{\cos \frac{\theta}{2}}{\sqrt{2}} \begin{bmatrix} 1 \\ -1 \end{bmatrix} + \frac{ie^{-i\varphi} \sin \frac{\theta}{2}}{\sqrt{2}} \begin{bmatrix} 1 \\ 1 \end{bmatrix}, \\ |\phi^\perp(\theta, \varphi)\rangle &= \frac{\cos \frac{\theta}{2}}{\sqrt{2}} \begin{bmatrix} 1 \\ 1 \end{bmatrix} + \frac{ie^{i\varphi} \sin \frac{\theta}{2}}{\sqrt{2}} \begin{bmatrix} 1 \\ -1 \end{bmatrix}, \end{aligned} \quad (19)$$

with the eigenvalues $E = r$ and $E^\perp = -r$, respectively. Assume that the initial value of θ is zero and the initial state of the qubit q is $(|e\rangle_q - |g\rangle_q)/\sqrt{2}$. The qubit q will evolve along the path $|\phi\rangle$ under the adiabatic limit $|\dot{\theta}|, |\dot{\varphi}| \ll |E - E^\perp| = 2r$ [86,87]. According to Eq. (10), the components of the Berry connection along the path $|\phi\rangle$ can be calculated by [67]

$$A_\theta = i\langle\phi|\frac{\partial}{\partial\theta}|\phi\rangle = 0, \quad A_\varphi = i\langle\phi|\frac{\partial}{\partial\varphi}|\phi\rangle = \sin^2 \frac{\theta}{2}. \quad (20)$$

According to Eq. (12), the Berry curvature can be derived from the Berry connection as

$$B_{\theta\varphi} = \frac{\partial}{\partial\theta} A_\varphi - \frac{\partial}{\partial\varphi} A_\theta = \frac{\sin \theta}{2}. \quad (21)$$

According to Eq. (13), by integrating the Berry curvature over a parametric manifold \mathcal{S}_q with $\theta \in [0, \pi]$ and $\varphi \in [0, 2\pi]$, we obtain a topological invariant, i.e., the Chern number in the odd-parity case as

$$\mathcal{C}_o = \frac{1}{2\pi} \iint_{\mathcal{S}_q} B_{\theta\varphi} d\theta d\varphi = \frac{1}{2\pi} \int_0^{2\pi} d\varphi \int_0^\pi \frac{\sin \theta}{2} d\theta = 1. \quad (22)$$

This result implies that the parametric manifold S_q is topological nontrivial when the cat-state qubits 1 and 2 are in the odd-parity state.

D. The Chern number in the even-parity case

To illustrate the evolution of the qubit q in the even-parity case, we first consider the case that the cat-state qubits 1 and 2 are in the state $|\tilde{\Psi}_+\rangle_{1,2}$ after the Hadamard gates $\{\mathcal{H}_n|n=1,2\}$ in Eq. (15), where $|\tilde{\Psi}_+\rangle_{1,2}$ is a component of the vector $|\Phi_e\rangle$ in Eq. (16). According to the effective Hamiltonian H_{eff} in Eq. (8) and the parametrization in Eq. (17), assuming $r\lambda = -2g\alpha^*$, the evolution of the qubit q is governed by the Hamiltonian

$$H_{q,e} = -r(\lambda + \cos\theta)\sigma_x + r\sin\theta\cos\varphi\sigma_y + r\sin\theta\sin\varphi\sigma_z. \quad (23)$$

The eigenvectors of the Hamiltonian $H_{q,e}$ in Eq. (23) are

$$|\tilde{\phi}(\theta, \varphi)\rangle = |\phi(\tilde{\theta}, \varphi)\rangle, \quad |\tilde{\phi}^\perp(\theta, \varphi)\rangle = |\phi^\perp(\tilde{\theta}, \varphi)\rangle, \quad (24)$$

with the eigenvalues

$$\begin{aligned} \tilde{E} &= r\sqrt{1 + \lambda^2 + 2\lambda\cos\theta}, \\ \tilde{E}^\perp &= -r\sqrt{1 + \lambda^2 + 2\lambda\cos\theta}, \end{aligned} \quad (25)$$

respectively. Here, the angle $\tilde{\theta}$ is a function of θ , which can be obtained by solving

$$\begin{aligned} \cos\tilde{\theta} &= \frac{\lambda + \cos\theta}{\sqrt{1 + \lambda^2 + 2\lambda\cos\theta}}, \\ \sin\tilde{\theta} &= \frac{\sin\theta}{\sqrt{1 + \lambda^2 + 2\lambda\cos\theta}}. \end{aligned} \quad (26)$$

Consider that the initial state of the qubit q is $(|e\rangle_q - |g\rangle_q)/\sqrt{2}$ with $\theta|_{t=0} = 0$. The qubit q will evolve along the path $|\tilde{\phi}\rangle$ under the adiabatic limit $|\dot{\theta}|, |\dot{\varphi}| \ll |\tilde{E} - \tilde{E}^\perp| = 2r\sqrt{1 + \lambda^2 + 2\lambda\cos\theta}$ [86,87]. According to Eq. (10), the components of the Berry connection along the path $|\tilde{\phi}\rangle$ can be calculated by

$$\tilde{A}_\theta = i\frac{d\tilde{\theta}}{d\theta}\langle\tilde{\phi}|\frac{\partial}{\partial\tilde{\theta}}|\tilde{\phi}\rangle = 0, \quad \tilde{A}_\varphi = i\langle\tilde{\phi}|\frac{\partial}{\partial\varphi}|\tilde{\phi}\rangle = \sin^2\frac{\tilde{\theta}}{2}, \quad (27)$$

and the corresponding Berry curvature is

$$\tilde{B}_{\theta\varphi} = \frac{\partial}{\partial\theta}\tilde{A}_\varphi - \frac{\partial}{\partial\varphi}\tilde{A}_\theta = \frac{\sin\tilde{\theta}}{2}\frac{d\tilde{\theta}}{d\theta}, \quad (28)$$

according to Eq. (12). According to Eq. (13), the Chern number in this case is

$$\begin{aligned} \mathcal{C}_e &= \frac{1}{2\pi} \iint_{S_q} \tilde{B}_{\theta\varphi} d\theta d\varphi \\ &= \frac{1}{2\pi} \int_0^{2\pi} d\varphi \int_0^\pi \frac{\sin\tilde{\theta}}{2} \frac{d\tilde{\theta}}{d\theta} d\theta \\ &= \int_{\tilde{\theta}(0)}^{\tilde{\theta}(\pi)} \frac{\sin\tilde{\theta}}{2} d\tilde{\theta} = \frac{\cos\tilde{\theta}}{2} \Big|_{\tilde{\theta}(0)}^{\tilde{\theta}(\pi)}. \end{aligned} \quad (29)$$

If $|\lambda| < 1$, we derive $\tilde{\theta}(0) = 0$ and $\tilde{\theta}(\pi) = \pi$ from Eq. (26), and the Chern number remains 1, while for $\lambda > 1$ ($\lambda <$

-1), we have $\tilde{\theta}(0) = \tilde{\theta}(\pi) = 0$ [$\tilde{\theta}(0) = \tilde{\theta}(\pi) = \pi$], yielding $\mathcal{C}_e = 0$. This implies that a topological phase transition is induced by the resonator-qubit couplings when $|\lambda| > 1$.

According to the effective Hamiltonian H_{eff} in Eq. (8), by replacing the parameter as $r\lambda = 2g\alpha^*$, the results above can also be applied to the case that the cat-state qubits 1 and 2 are in the state $|\tilde{\Psi}_-\rangle_{1,2}$ after the Hadamard gates $\{\mathcal{H}_n|n=1,2\}$ in Eq. (15), where $|\tilde{\Psi}_-\rangle_{1,2}$ is also a component of the vector $|\Phi_e\rangle$ in Eq. (16). Because the vector $|\Phi_e\rangle$ is a linear superposition of the vectors $\{|\tilde{\Psi}_\pm\rangle_{1,2}\}$, the above results can be extended to the whole even-parity case.

E. Measurement of the Berry curvature and the Chern number through a generalized force

We define a generalized force $f_\varphi = -\partial_\varphi \tilde{H}_q$, where \tilde{H}_q denotes the Hamiltonian of the qubit q with $\tilde{H}_q = H_{q,o}$ in Eq. (18) [$\tilde{H}_q = H_{q,e}$ in Eq. (23)] in the odd-parity (even-parity) case. According to the results reported in Refs. [61,62], when the parameter φ is time independent, the Berry curvature can be experimentally measured through the relation

$$\langle f_\varphi \rangle = \langle \tilde{\phi} | f_\varphi | \tilde{\phi} \rangle - v_\theta \bar{B}_{\theta\varphi} + O(v_\theta^2), \quad (30)$$

with the eigenvector $|\tilde{\phi}\rangle$ of the Hamiltonian \tilde{H}_q used as the evolution path, the variation speed $v_\theta = \dot{\theta}$ of the parameter θ in an adiabatic evolution, and the Berry curvature $\bar{B}_{\theta\varphi}$ related to the path $|\tilde{\phi}\rangle$. In the present scheme, we have $f_\varphi = r\sin\theta(\sin\varphi\sigma_y - \cos\varphi\sigma_z)$ for both the odd- and even-parity cases. In addition, the result $\langle \tilde{\phi} | f_\varphi | \tilde{\phi} \rangle = 0$ can be obtained by substituting $|\tilde{\phi}\rangle = |\phi\rangle$ or $|\tilde{\phi}\rangle = |\phi^\perp\rangle$. Using Eq. (30), the Berry curvature can be estimated by

$$\bar{B}_{\theta\varphi} \simeq -\frac{1}{v_\theta} \langle f_\varphi \rangle = -\frac{1}{v_\theta} \left\{ \frac{\Delta(t)}{2} \langle \sigma_y \rangle - \text{Im}[\Omega(t)] \langle \sigma_z \rangle \right\}. \quad (31)$$

According to Eqs. (21) and (28), the Berry curvature $\bar{B}_{\theta\varphi}$ is independent of the parameter φ . Hence, one can measure the Berry curvature by selecting an arbitrary φ . For example, when $\varphi = 0$ is considered, we have

$$\bar{B}_{\theta\varphi} \simeq -\frac{1}{v_\theta} \langle f_\varphi \rangle|_{\varphi=0} = \frac{1}{v_\theta} \text{Im}[\Omega(t)] \langle \sigma_z \rangle. \quad (32)$$

Using the cylindrical symmetry of $\bar{B}_{\theta\varphi}$, the Chern number can be obtained from the integral [62]

$$\mathcal{C} = \int_0^\pi \bar{B}_{\theta\varphi} d\theta. \quad (33)$$

To calculate the integral in Eq. (33), we can measure the average value $\langle \sigma_z \rangle$ with different values of θ along the evolution path $|\tilde{\phi}(\theta, 0)\rangle$ via state tomography [62] of the qubit q .

IV. NUMERICAL SIMULATIONS

To verify the scheme can be used to distinguish the parity of the cat-state qubits, we perform the numerical simulation with a set of available parameters $r = 2\pi \times 1.5$ MHz, $v_\theta = 2\pi \times 0.25$ MHz, $K_n = 2\pi \times 12.5$ MHz, and $\alpha = 2$ [88]. As the examples, the even-parity and the odd-parity states of the cat-state qubits being measured are selected as $|\Psi_e\rangle = |\Psi_+\rangle_{1,2}$ and $|\Psi_o\rangle = |\Psi_+\rangle_{1,2}$, respectively. We first consider the case

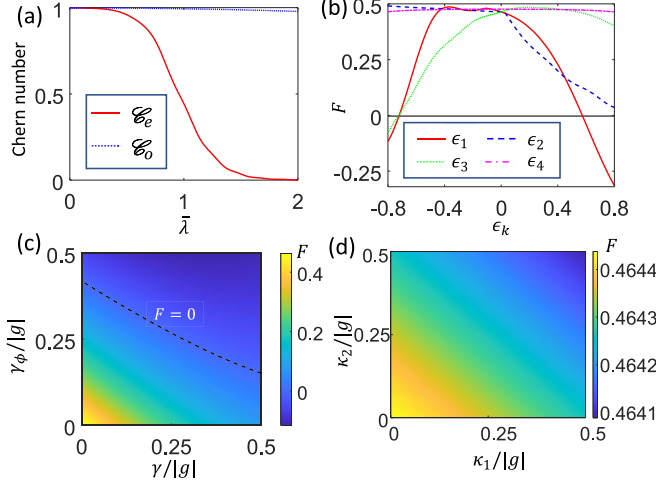


FIG. 2. (a) The measured Chern number vs $\bar{\lambda} = -2g\alpha/r$. (b) The evaluation criterion function F vs error coefficient ϵ_k ($k = 1, 2, 3, 4$) with $\bar{\lambda} = 1.5$. (c) The evaluation criterion function F vs $\gamma/|g|$ and $\gamma_\phi/|g|$ with $\bar{\lambda} = 1.5$. (d) The evaluation criterion function F vs $\kappa_1/|g|$ and $\kappa_2/|g|$ with $\bar{\lambda} = 1.5$. The parameters are $r = 2\pi \times 1.5$ MHz, $v_\theta = 2\pi \times 0.25$ MHz, $K_n = 2\pi \times 12.5$ MHz, and $\alpha = 2$.

that the Hadamard gates $\{\mathcal{H}_n | n = 1, 2\}$ in Eq. (15) are perfect. In this case, the even-parity and the odd-parity states of the cat-state qubits are transformed into $|\Phi_e\rangle = |\Psi_+\rangle_{1,2}$ and $|\Phi_o\rangle = |\Psi_-\rangle_{1,2}$, respectively.

A. Variations of the Chern numbers with the coupling strength

Based on Eqs. (32) and (33), the measured Chern number versus $\bar{\lambda} = -2g\alpha/r$ is plotted in Fig. 2(a). As shown by the figure, the Chern number \mathcal{C}_o remains near 1 in the odd-parity case, in accordance with the theoretical analysis. In the even-parity case, the Chern number is near 1 when $\bar{\lambda} < 1$ and tends to 0 sharply when $\bar{\lambda} > 1$. The result indicates that it is possible to distinguish the even-parity states from the odd-parity states when $\bar{\lambda} > 1$. However, when $\bar{\lambda}$ is very close to 1, the measured Chern number is between 0 and 1, because the adiabatic condition $v_\theta \ll r(1 + \bar{\lambda}^2 + 2\bar{\lambda} \cos \theta)^{1/2}$ can hardly be satisfied during the whole evolution. Especially for $\bar{\lambda} = 1$ and $\theta = \pi$, we have $r(1 + \bar{\lambda}^2 + 2\bar{\lambda} \cos \theta)^{1/2} = 0$, i.e., it is a degenerate point for the eigenvectors $|\phi\rangle$ and $|\phi^\perp\rangle$ in Eq. (24). Therefore, for a better discrimination between the different parities in an experiment, the value of $\bar{\lambda}$ should not be too close to the critical point $\bar{\lambda} = 1$. For example, when $\bar{\lambda} = 1.5$, the Chern numbers in the odd- and even-parity cases are $\mathcal{C}_o = 0.9877$ and $\mathcal{C}_e = 0.0356$, respectively. The odd-parity states and the even-parity states can be well distinguished. Even when $\bar{\lambda} = 1.25$, where the Chern numbers are $\mathcal{C}_o = 0.9912$ and $\mathcal{C}_e = 0.1501$, the two parities can be still well distinguished. If we consider that the measurement results with $\mathcal{C} > 0.5$ and $\mathcal{C} < 0.5$ respectively correspond to the odd- and even-parity cases, the scheme can still succeed when $\bar{\lambda} = 0.9566$. The above results demonstrate that the scheme has great tolerance for the deviation of the resonator-qubit coupling strengths.

In practice, to estimate the performance of the scheme in the presence of other disturbing factors, we can define an evaluation criterion function as $F = \min\{\mathcal{C}_o - 0.5, 0.5 - \mathcal{C}_e\}$. $F > 0$ means that the scheme is successful, while $F < 0$ declares that the scheme fails.

B. Influence of the systematic errors and the inter-resonator crosstalk

We first consider the following four disturbing factors: (i) the systematic error of the real part $\text{Re}[\Omega(t)] \rightarrow (1 + \epsilon_1)\text{Re}[\Omega(t)]$ of the Rabi frequency with the error coefficient ϵ_1 , (ii) the systematic error of the imaginary part $\text{Im}[\Omega(t)] \rightarrow (1 + \epsilon_2)\text{Im}[\Omega(t)]$ of the Rabi frequency with the error coefficient ϵ_2 , (iii) the systematic error of the coupling strength $g_1 \rightarrow (1 + \epsilon_3)g_1$ with the error coefficient ϵ_3 , and (iv) the inter-resonator crosstalk with the Hamiltonian $H_{ct} = \epsilon_4 g(a_1^\dagger a_2 + a_1 a_2^\dagger)$ and error coefficient ϵ_4 . Here, as the Chern number is measured along the path with $\varphi = 0$, $\Delta(t) = 0$ is obtained in this case. Thus, the systematic error of the detuning $\Delta(t)$ is not considered. In addition, we have shown that the scheme has great tolerance for the deviation of the coupling strengths in the case of $g_1 = g_2$ in Fig. 2(a). Without loss of generality, we here only consider the systematic error of the coupling strength g_1 , because the two coupling strengths are symmetric.

The evaluation criterion function F versus error coefficient ϵ_k ($k = 1, 2, 3, 4$) is shown in Fig. 2(b) with $\bar{\lambda} = 1.5$. According to the red-solid curve, we find that F remains positive in the range $\epsilon_1 \in [-0.72, 0.56]$. This means the scheme can still succeed even when the systematic error of the real part $\text{Re}[\Omega(t)]$ of the Rabi frequency reaches 50% of the original value. The blue-dashed curve in Fig. 2(b) shows that F is always positive in the range $\epsilon_2 \in [-0.8, 0.8]$. Consequently, the scheme can still succeed even when the systematic error of the imaginary part $\text{Im}[\Omega(t)]$ of the Rabi frequency reaches 80% of the original value. From the green-dotted curve in Fig. 2(b), one can see that F remains positive in the range $\epsilon_3 \in [-0.72, 0.8]$. The result indicates that the scheme can tolerate the systematic error of the coupling strength g_1 even when it reaches 70% of the original value. As shown by the magenta dash-dotted curve in Fig. 2(b), F is almost unchanged when ϵ_4 varies from -0.8 to 0.8 . The minimal value of F for the range $\epsilon_4 \in [-0.8, 0.8]$ is 0.4644, very close to the ideal value $F = 0.5$. This proves that the scheme is highly insensitive to the inter-resonator crosstalk. Recalling the result $a_n \simeq \alpha \sigma_{x,n}$, we derive $H_{ct} \simeq \epsilon_4 g |\alpha|^2 \sigma_{x,1} \sigma_{x,2}$. According to Eq. (16), $|\Phi_e\rangle$ and $|\Phi_o\rangle$ are the eigenvectors of H_{ct} with the eigenvalues 1 and -1 , respectively. Thus, the parity of the cat-state qubits can still be well preserved in the presence of the inter-resonator crosstalk. To sum up, the results of Fig. 2(b) demonstrate the scheme possesses perfect error tolerance for the systematic errors of different control parameters and the inter-resonator crosstalk.

C. Influence of the decoherence in the parity measurement

We also examine the performance of the scheme in the presence of decoherence. The main decoherence factors here are the energy relaxation of the level $|e\rangle_q$ of the qubit q with relaxation rate γ , the dephasing of the level $|e\rangle_q$ of the qubit q with the dephasing rate γ_ϕ , and the decay of the resonator C_n with the decay rate κ_n . The system under the influence of the

decoherence is governed by the master equation [89,90]

$$\dot{\rho} = -i[H_{\text{tot}}, \rho] + \frac{\gamma}{2}\mathcal{L}[|g\rangle_q\langle e|]\rho + \frac{\gamma_\phi}{2}\mathcal{L}[|e\rangle_q\langle e|]\rho + \sum_{n=1}^2 \frac{\kappa_n}{2}\mathcal{L}[a_n]\rho, \quad (34)$$

with the density operator ρ of the system and the Lindblad superoperator $\mathcal{L}[X]\rho = 2X\rho X^\dagger - X^\dagger X\rho - \rho X^\dagger X$ ($X = |g\rangle_q\langle e|, |e\rangle_q\langle e|, a_n$). The evaluation criterion function F versus γ/g and γ_ϕ/g (κ_1/g and κ_2/g) is plotted in Fig. 2(c) [Fig. 2(d)]. As shown in Fig. 2(c), the scheme is insensitive to the energy relaxation and the dephasing of the qubit q . When $\gamma_\phi \leqslant 0.152|g|$, the scheme can always succeed with $\gamma/|g| \in [0, 0.5]$. When $\gamma = 0$, the scheme can still succeed when $\gamma_\phi = 0.418|g|$. For $\gamma = \gamma_\phi = 0.25|g|$, we have $F = 0.0114 > 0$. The above results indicate that the protocol can still work when the energy relaxation rate and the dephasing rate of the qubit q are comparable with the coupling strength. According to Fig. 2(d), when κ_n varies from 0 to 0.5|g|, F is almost unchanged. Thus, the scheme is almost unaffected by the resonator decay when the Hadamard gates $\{\mathcal{H}_n|n = 1, 2\}$ are assumed to be perfect. This is due to the results $a_n \simeq \alpha\sigma_{x,n}$ and $\langle\Phi_e|a_n|\Phi_o\rangle \simeq 0$. Hence, the parity information is almost unaffected by the resonator decay during the parity measurement.

D. Influence of the imperfect Hadamard gates

In the above discussions, we considered that the Hadamard gates $\{\mathcal{H}_n|n = 1, 2\}$ in Eq. (15) are perfect. Let us now investigate the influence of the imperfect Hadamard gates $\{\mathcal{H}_n\}$ in the presence of the disturbing factors. Here, the strength of the linear drive used in the Hadamard gate is set as $\varsigma_n = 2\pi \times 5$ MHz, satisfying the condition $|\varsigma_n\alpha| \ll E_{\text{gap}}$ with $\alpha = 2$. For $r = 2\pi \times 1.5$ MHz, $v_\theta = 2\pi \times 0.25$ MHz, $K_n = 2\pi \times 12.5$ MHz, and $\bar{\lambda} = 1.5$, the total operation time for the Hadamard gate \mathcal{H}_n is $\tau_H = 32.5$ ns, and we have $\mathcal{C}_o = 0.9876$, $\mathcal{C}_e = 0.0360$, and $F = 0.4640$. When the systematic error of the linear drive is considered, the strength becomes $\varsigma_n \rightarrow (1 + \bar{\epsilon}_1)\varsigma_n$ with error coefficient $\bar{\epsilon}_1$. In addition, the systematic error of the frequency shift δ_n can be described by $\delta_n \rightarrow (1 + \bar{\epsilon}_2)\delta_n$ with error coefficient $\bar{\epsilon}_2$. The evaluation criterion function F versus error coefficient $\bar{\epsilon}_{k'} (k' = 1, 2)$ is shown in Fig. 3(a). From the figure, we find that F remains positive for $\bar{\epsilon}_1 \in [-0.49, 0.49]$. The result indicates that the scheme can still succeed even when the systematic error of the linear drive ς_n approaches about 50% of the original value. Accordingly, the scheme is insensitive to the systematic errors of the linear drive ς_n . For the systematic error of the frequency shift δ_n , we have $F > 0$ with $\bar{\epsilon}_2 \in [-0.214, 0.217]$. This means that the scheme can tolerate the systematic error of the frequency shift δ_n even when it is about 20% of the original value. The above result demonstrates that the scheme is also insensitive to the systematic errors of the frequency shift δ_n .

E. Influence of the resonator decay to the whole operation

Finally, we study the influence of the resonator decay to the whole operation including the Hadamard gates $\{\mathcal{H}_n|n = 1, 2\}$

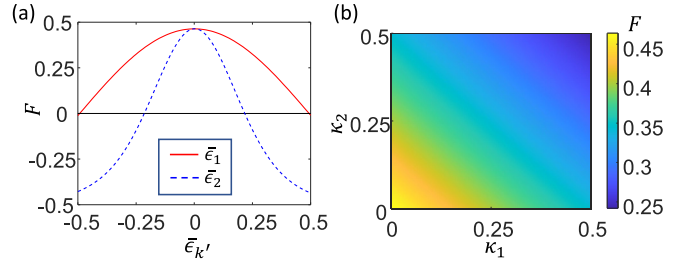


FIG. 3. (a) The evaluation criterion function F vs error coefficient $\bar{\epsilon}_{k'} (k' = 1, 2)$. (b) The evaluation criterion function F vs $\kappa_1/|g|$ and $\kappa_2/|g|$ when the Hadamard gates $\{\mathcal{H}_n|n = 1, 2\}$ are included. The parameters are $r = 2\pi \times 1.5$ MHz, $v_\theta = 2\pi \times 0.25$ MHz, $\bar{\lambda} = 1.5$, $K_n = 2\pi \times 12.5$ MHz, and $\alpha = 2$.

in Eq. (15). The evaluation criterion function F versus $\kappa_1/|g|$ and $\kappa_2/|g|$ is plotted in Fig. 3(b). As shown by Fig. 3(b), at the same point of $(\kappa_1/|g|, \kappa_2/|g|)$, the evaluation criterion function F is reduced compared with the results given in Fig. 2(d). This is because the resonator C_n first evolves out from the cat-state subspace and then evolves back into the cat-state subspace during the operation U_2 in the Hadamard gate \mathcal{H}_n . When the state of the resonator C_n is not in the cat-state subspace, the parity information is unprotected and may lose due to the resonator decay. Nevertheless, F still remains positive for $\kappa_1 \leqslant 0.5|g|$ and $\kappa_2 \leqslant 0.5|g|$ when the Hadamard gates $\{\mathcal{H}_n|n = 1, 2\}$ are considered. The minimal value of F in the considered ranges of the resonator decay rates is $F = 0.2420$. Consequently, the scheme can still succeed when the resonator decay in the Hadamard gates $\{\mathcal{H}_n|n = 1, 2\}$ is taken into account, even with the resonator decay rates κ_1 and κ_2 comparable with the resonator-qubit coupling strength g .

V. CONCLUSION

We have proposed a scheme to construct a parity detector of cat-state qubits based on a topological quantum phase transition. The cat-state qubits are formed by the bosonic modes in the Kerr-nonlinear resonators driven by the two-photon squeezing drives. The resonators couple with a superconducting qubit in the center. Tuning resonator-qubit coupling strengths, one can realize a topological quantum phase transition when the cat-state qubits are initial in the even-parity states. This phenomenon can be applied to distinguish the even-parity states from the odd-parity states by measuring the Chern number. Because of the robustness of the Chern number, the scheme is insensitive to different kinds of disturbing factors, including the systematic errors of the control fields and the coupling strengths, the inter-resonator crosstalk, and decoherence. Therefore, the scheme may provide useful perspectives for the error-tolerant parity measurement of cat-state qubits.

ACKNOWLEDGMENTS

This work was supported by National Natural Science Foundation of China under Grants No. 11374083, No. 11774076, No. 12204139, No. 12205069, and

No. U21A20436, and the Innovation Program for Quantum Science and Technology under Grant No. 2021ZD0301705.

APPENDIX: REALIZATION OF THE HADAMARD GATE OF THE CAT-STATE QUBIT

Let us show the realization of the Hadamard gate \mathcal{H}_n in Eq. (15) of the cat-state qubit n in the Kerr-nonlinear resonator C_n . To realize the Hadamard gate \mathcal{H}_n , we apply a linear drive to the resonator C_n as $H_{l,n} = \varsigma_n^* a_n + \varsigma_n a_n^\dagger$ with the strength ς_n . When $|\varsigma_n \alpha| \ll E_{\text{gap}}$ is satisfied, we have $H_{l,n} \simeq 2\text{Re}[\varsigma_n \alpha^*] \sigma_{x,n}$. For the operation time $t = \pi/8\text{Re}[\varsigma_n \alpha^*]$, it leads to a transformation in the cat-state subspace $\mathcal{S}_{c,n} = \text{span}\{|\mathcal{C}_\pm\rangle_n\}$ as

$$U_1 = \frac{1}{\sqrt{2}} \begin{bmatrix} 1 & -i \\ -i & 1 \end{bmatrix}. \quad (\text{A1})$$

Then, we turn off the two-photon squeezing drive ε_n and the linear drive ς_n , and tune the frequency of the resonator C_n

from ω_n to $\omega_n - \delta_n$. In the frame rotating at the frequency ω_n , the Hamiltonian of the resonator C_n reads

$$H'_n = -K_n a_n^\dagger a_n - \delta_n a_n^\dagger a_n. \quad (\text{A2})$$

Under the condition $\delta_n = K_n$ and the operation time $t = \pi/2K_n$, one can realize a transformation in the cat-state subspace $\mathcal{S}_{c,n}$ as

$$U_2 = \begin{bmatrix} 1 & 0 \\ 0 & i \end{bmatrix}. \quad (\text{A3})$$

Finally, we tune the frequency of the resonator back to ω_n and repeat the operation U_1 ; the total operation for the system in the cat-state subspace $\mathcal{S}_{c,n}$ can be described as

$$U_{\text{tot}} = U_1 U_2 U_1 = \frac{e^{-i\frac{\pi}{4}}}{\sqrt{2}} \begin{bmatrix} 1 & 1 \\ 1 & -1 \end{bmatrix}, \quad (\text{A4})$$

which is equivalent to the Hadamard gate \mathcal{H}_n in Eq. (15) for the cat-state qubit n up to a global phase $-\pi/4$.

-
- [1] H.-A. Engel and D. Loss, *Science* **309**, 586 (2005).
 - [2] D. P. DiVincenzo and F. Solgun, *New J. Phys.* **15**, 075001 (2013).
 - [3] L. Sun, A. Petrenko, Z. Leghtas, B. Vlastakis, G. Kirchmair, K. M. Sliwa, A. Narla, M. Hatridge, S. Shankar, J. Blumoff, L. Frunzio, M. Mirrahimi, M. H. Devoret, and R. J. Schoelkopf, *Nature (London)* **511**, 444 (2014).
 - [4] O.-P. Saira, J. P. Groen, J. Cramer, M. Meretska, G. de Lange, and L. DiCarlo, *Phys. Rev. Lett.* **112**, 070502 (2014).
 - [5] P.-S. Yan, L. Zhou, W. Zhong, and Y.-B. Sheng, *Sci. China Phys. Mech. Astron.* **66**, 250301 (2023).
 - [6] J. Miguel-Ramiro, F. Riera-Sàbat, and W. Dür, *PRX Quantum* **4**, 040323 (2023).
 - [7] C. W. J. Beenakker, D. P. DiVincenzo, C. Emery, and M. Kindermann, *Phys. Rev. Lett.* **93**, 020501 (2004).
 - [8] K. Nemoto and W. J. Munro, *Phys. Rev. Lett.* **93**, 250502 (2004).
 - [9] C. Bonato, F. Haupt, S. S. R. Oemrawsingh, J. Gudat, D. Ding, M. P. van Exter, and D. Bouwmeester, *Phys. Rev. Lett.* **104**, 160503 (2010).
 - [10] J.-W. Pan, D. Bouwmeester, H. Weinfurter, and A. Zeilinger, *Phys. Rev. Lett.* **80**, 3891 (1998).
 - [11] M. Halder, A. Beveratos, N. Gisin, V. Scarani, C. Simon, and H. Zbinden, *Nat. Phys.* **3**, 692 (2007).
 - [12] W. Ning, X.-J. Huang, P.-R. Han, H. Li, H. Deng, Z.-B. Yang, Z.-R. Zhong, Y. Xia, K. Xu, D. Zheng, and S.-B. Zheng, *Phys. Rev. Lett.* **123**, 060502 (2019).
 - [13] C. H. Bennett, G. Brassard, C. Crépeau, R. Jozsa, A. Peres, and W. K. Wootters, *Phys. Rev. Lett.* **70**, 1895 (1993).
 - [14] A. Karlsson and M. Bourennane, *Phys. Rev. A* **58**, 4394 (1998).
 - [15] F.-Q. Guo, J.-L. Wu, X.-Y. Zhu, Z. Jin, Y. Zeng, S. Zhang, L.-L. Yan, M. Feng, and S.-L. Su, *Phys. Rev. A* **102**, 062410 (2020).
 - [16] J.-W. Pan, C. Simon, V. Brukner, and A. Zeilinger, *Nature (London)* **410**, 1067 (2001).
 - [17] Y.-B. Sheng and F.-G. Deng, *Phys. Rev. A* **81**, 032307 (2010).
 - [18] P.-S. Yan, L. Zhou, W. Zhong, and Y.-B. Sheng, *Phys. Rev. A* **105**, 062418 (2022).
 - [19] J. Qi, K. Li, Z. Yang, R.-Y. Yuan, and B.-C. Ren, *Phys. Rev. A* **109**, 042423 (2024).
 - [20] D. Ristè, M. Dukalski, C. A. Watson, G. de Lange, M. J. Tiggelman, Y. M. Blanter, K. W. Lehnert, R. N. Schouten, and L. DiCarlo, *Nature (London)* **502**, 350 (2013).
 - [21] B. M. Terhal, *Rev. Mod. Phys.* **87**, 307 (2015).
 - [22] K. Azuma, S. E. Economou, D. Elkouss, P. Hilaire, L. Jiang, H.-K. Lo, and I. Tzitrin, *Rev. Mod. Phys.* **95**, 045006 (2023).
 - [23] Y.-B. Sheng, F.-G. Deng, and G. L. Long, *Phys. Rev. A* **82**, 032318 (2010).
 - [24] K. Azuma, H. Takeda, M. Koashi, and N. Imoto, *Phys. Rev. A* **85**, 062309 (2012).
 - [25] S.-L. Su, F.-Q. Guo, L. Tian, X.-Y. Zhu, L.-L. Yan, E.-J. Liang, and M. Feng, *Phys. Rev. A* **101**, 012347 (2020).
 - [26] R.-H. Zheng, Y.-H. Kang, S.-L. Su, J. Song, and Y. Xia, *Phys. Rev. A* **102**, 012609 (2020).
 - [27] S. B. van Dam, J. Cramer, T. H. Taminiau, and R. Hanson, *Phys. Rev. Lett.* **123**, 050401 (2019).
 - [28] B. Trauzettel, A. N. Jordan, C. W. J. Beenakker, and M. Büttiker, *Phys. Rev. B* **73**, 235331 (2006).
 - [29] M. Sisodia, A. Shukla, and A. Pathak, *Phys. Lett. A* **381**, 3860 (2017).
 - [30] Y. Xiao, Y.-H. Kang, R.-H. Zheng, Y. Liu, Y. Wang, J. Song, and Y. Xia, *Adv. Quantum Technol.* **6**, 2200192 (2023).
 - [31] E. Kapit, *Phys. Rev. Lett.* **120**, 050503 (2018).
 - [32] L. Hu, Y. Ma, W. Cai, X. Mu, Y. Xu, W. Wang, Y. Wu, H. Wang, Y. P. Song, C.-L. Zou, S. M. Girvin, L.-M. Duan, and L. Sun, *Nat. Phys.* **15**, 503 (2019).
 - [33] Y. Ma, Y. Xu, X. Mu, W. Cai, L. Hu, W. Wang, X. Pan, H. Wang, Y. P. Song, C.-L. Zou, and L. Sun, *Nat. Phys.* **16**, 827 (2020).
 - [34] W. Cai, Y. Ma, W. Wang, C.-L. Zou, and L. Sun, *Fundam. Res.* **1**, 50 (2021).
 - [35] Q.-P. Su, L. Bin, Y. Zhang, and C.-P. Yang, *Phys. Rev. A* **107**, 032616 (2023).
 - [36] B. J. Chapman, S. J. de Graaf, S. H. Xue, Y. Zhang, J. Teoh, J. C. Curtis, T. Tsunoda, A. Eickbusch, A. P. Read, A. Koottandavida, S. O. Mundhada, L. Frunzio, M. H. Devoret,

- S. M. Girvin, and R. J. Schoelkopf, *PRX Quantum* **4**, 020355 (2023).
- [37] Z. Li, T. Roy, D. Rodríguez Pérez, K.-H. Lee, E. Kapit, and D. I. Schuster, *Nat. Commun.* **15**, 1681 (2024).
- [38] S. Puri, A. Grimm, P. Campagne-Ibarcq, A. Eickbusch, K. Noh, G. Roberts, L. Jiang, M. Mirrahimi, M. H. Devoret, and S. M. Girvin, *Phys. Rev. X* **9**, 041009 (2019).
- [39] Y.-H. Chen, W. Qin, X. Wang, A. Miranowicz, and F. Nori, *Phys. Rev. Lett.* **126**, 023602 (2021).
- [40] C. Chamberland, K. Noh, P. Arrangoiz-Arriola, E. T. Campbell, C. T. Hann, J. Iverson, H. Puterman, T. C. Bohdanowicz, S. T. Flammia, A. Keller, G. Refael, J. Preskill, L. Jiang, A. H. Safavi-Naeini, O. Painter, and F. G. S. L. Brandão, *PRX Quantum* **3**, 010329 (2022).
- [41] L. Gravina, F. Minganti, and V. Savona, *PRX Quantum* **4**, 020337 (2023).
- [42] C.-P. Yang, J.-H. Ni, L. Bin, Y. Zhang, Y. Yu, and Q.-P. Su, *Front. Phys.* **19**, 31201 (2023).
- [43] T. Aoki, T. Kanao, H. Goto, S. Kawabata, and S. Masuda, *Phys. Rev. Appl.* **21**, 014030 (2024).
- [44] M. Mirrahimi, Z. Leghtas, V. V. Albert, S. Touzard, R. J. Schoelkopf, L. Jiang, and M. H. Devoret, *New J. Phys.* **16**, 045014 (2014).
- [45] J. Guillaud and M. Mirrahimi, *Phys. Rev. X* **9**, 041053 (2019).
- [46] A. Marquet, A. Essig, J. Cohen, N. Cottet, A. Murani, E. Albertinale, S. Dupouy, A. Bienfait, T. Peronnin, S. Jezouin, R. Lescanne, and B. Huard, *Phys. Rev. X* **14**, 021019 (2024).
- [47] U. Réglade, A. Bocquet, R. Gautier, J. Cohen, A. Marquet, E. Albertinale, N. Pankratova, M. Hallén, F. Rautschke, L.-A. Sellem, P. Rouchon, A. Sarlette, M. Mirrahimi, P. Campagne-Ibarcq, R. Lescanne, S. Jezouin, and Z. Leghtas, *Nature (London)* **629**, 778 (2024).
- [48] V. V. Albert, C. Shu, S. Krastanov, C. Shen, R.-B. Liu, Z.-B. Yang, R. J. Schoelkopf, M. Mirrahimi, M. H. Devoret, and L. Jiang, *Phys. Rev. Lett.* **116**, 140502 (2016).
- [49] Y. Xu, Y. Ma, W. Cai, X. Mu, W. Dai, W. Wang, L. Hu, X. Li, J. Han, H. Wang, Y. P. Song, Z.-B. Yang, S.-B. Zheng, and L. Sun, *Phys. Rev. Lett.* **124**, 120501 (2020).
- [50] Q.-P. Su, Y. Zhang, and C.-P. Yang, *Phys. Rev. A* **105**, 062436 (2022).
- [51] Y.-H. Kang, Y.-H. Chen, X. Wang, J. Song, Y. Xia, A. Miranowicz, S.-B. Zheng, and F. Nori, *Phys. Rev. Res.* **4**, 013233 (2022).
- [52] T. Kanao, S. Masuda, S. Kawabata, and H. Goto, *Phys. Rev. Appl.* **18**, 014019 (2022).
- [53] T. Kanao and H. Goto, *Phys. Rev. Res.* **6**, 013192 (2024).
- [54] D.-S. Li, Y.-H. Kang, X.-Y. Zhao, J. Song, and Y. Xia, *Ann. Phys. (Leipzig)* **535**, 2200483 (2023).
- [55] D.-S. Li, Y.-H. Kang, Y.-H. Chen, Y. Liu, C. Zhang, Y. Wang, J. Song, and Y. Xia, *Phys. Rev. A* **109**, 022437 (2024).
- [56] F. A. Hashmi and M. A. Bouchene, *Phys. Rev. A* **79**, 025401 (2009).
- [57] A. Ruschhaupt, X. Chen, D. Alonso, and J. G. Muga, *New J. Phys.* **14**, 093040 (2012).
- [58] D. J. Thouless, M. Kohmoto, M. P. Nightingale, and M. den Nijs, *Phys. Rev. Lett.* **49**, 405 (1982).
- [59] Q. Niu, D. J. Thouless, and Y.-S. Wu, *Phys. Rev. B* **31**, 3372 (1985).
- [60] Y. Hatsugai, *Phys. Rev. Lett.* **71**, 3697 (1993).
- [61] V. Gritsev and A. Polkovnikov, *Proc. Natl. Acad. Sci. USA* **109**, 6457 (2012).
- [62] M. D. Schroer, M. H. Kolodrubetz, W. F. Kindel, M. Sandberg, J. Gao, M. R. Vissers, D. P. Pappas, A. Polkovnikov, and K. W. Lehnert, *Phys. Rev. Lett.* **113**, 050402 (2014).
- [63] E. Bernhardt, C. Elouard, and K. Le Hur, *Phys. Rev. A* **107**, 022219 (2023).
- [64] S. Puri, S. Boutin, and A. Blais, *npj Quantum Inf.* **3**, 18 (2017).
- [65] Z. Wang, M. Pechal, E. A. Wollack, P. Arrangoiz-Arriola, M. Gao, N. R. Lee, and A. H. Safavi-Naeini, *Phys. Rev. X* **9**, 021049 (2019).
- [66] A. Grimm, N. E. Frattini, S. Puri, S. O. Mundhada, S. Touzard, M. Mirrahimi, S. M. Girvin, S. Shankar, and M. H. Devoret, *Nature (London)* **584**, 205 (2020).
- [67] M. V. Berry, *Proc. R. Soc. A* **392**, 45 (1984).
- [68] S. Sugawa, F. Salces-Carcoba, A. R. Perry, Y. Yue, and I. B. Spielman, *Science* **360**, 1429 (2018).
- [69] S.-s. Chern, *Ann. Math.* **47**, 85 (1946).
- [70] J. K. Asbóth, L. Oroszlány, and A. Pályi, Berry phase, Chern number, *A Short Course on Topological Insulators*, Lecture Notes in Physics, Vol. 919 (Springer, Cham, 2016), pp. 23–44.
- [71] P. Deng, P. Zhang, C. Eckberg, S. K. Chong, G. Yin, E. Emmanouilidou, X. Che, N. Ni, and K. L. Wang, *Nat. Commun.* **14**, 5558 (2023).
- [72] F. D. M. Haldane, *Phys. Rev. Lett.* **93**, 206602 (2004).
- [73] Y. Zhang, Y.-W. Tan, H. L. Stormer, and P. Kim, *Nature (London)* **438**, 201 (2005).
- [74] A. Tomita and R. Y. Chiao, *Phys. Rev. Lett.* **57**, 937 (1986).
- [75] D. J. Thouless, *Phys. Rev. B* **27**, 6083 (1983).
- [76] Q. Niu and D. J. Thouless, *J. Phys. A* **17**, 2453 (1984).
- [77] S. A. Hassani Gangaraj, M. G. Silveirinha, and G. W. Hanson, *IEEE J. Multiscale Multiphys. Comput. Tech.* **2**, 3 (2017).
- [78] J. A. Jones, V. Vedral, A. Ekert, and G. Castagnoli, *Nature (London)* **403**, 869 (2000).
- [79] G. Falci, R. Fazio, G. M. Palma, J. Siewert, and V. Vedral, *Nature (London)* **407**, 355 (2000).
- [80] K. Mæland and A. Sudbø, *Phys. Rev. Res.* **4**, L032025 (2022).
- [81] Y. Wang, K. Snizhko, A. Romito, Y. Gefen, and K. Murch, *Phys. Rev. Res.* **4**, 023179 (2022).
- [82] J. Ge, Y. Liu, P. Wang, Z. Xu, J. Li, H. Li, Z. Yan, Y. Wu, Y. Xu, and J. Wang, *Phys. Rev. B* **105**, L201404 (2022).
- [83] B. Li, W. Sun, X. Zou, X. Li, B. Huang, Y. Dai, and C. Niu, *New J. Phys.* **24**, 053038 (2022).
- [84] R. R. Kumar, N. Roy, Y. R. Kartik, S. Rahul, and S. Sarkar, *Phys. Rev. B* **107**, 205114 (2023).
- [85] X.-Y. Song, C.-M. Jian, L. Fu, and C. Xu, *Phys. Rev. B* **109**, 115116 (2024).
- [86] P. Král, I. Thanopoulos, and M. Shapiro, *Rev. Mod. Phys.* **79**, 53 (2007).
- [87] D. Guéry-Odelin, A. Ruschhaupt, A. Kiely, E. Torrontegui, S. Martínez-Garaot, and J. G. Muga, *Rev. Mod. Phys.* **91**, 045001 (2019).
- [88] A. Vrajitoarea, Z. Huang, P. Groszkowski, J. Koch, and A. A. Houck, *Nat. Phys.* **16**, 211 (2019).
- [89] C.-P. Yang, Q.-P. Su, S.-B. Zheng, and F. Nori, *Phys. Rev. A* **93**, 042307 (2016).
- [90] Q.-P. Su, Y. Zhang, L. Bin, and C.-P. Yang, *Phys. Rev. A* **105**, 042434 (2022).